Fiber Bragg Gratings for Prognostics in Space Applications: A Thermo-Mechanical Characterization of Minimally Invasive Sensing Techniques

(Article begins on next page)

11 April 2024

FIBER BRAGG GRATINGS FOR PROGNOSTICS IN SPACE APPLICATIONS: A THERMO-MECHANICAL CHARACTERIZATION OF MINIMALLY INVASIVE SENSING TECHNIQUES

Pier Carlo Berri [(1)], Matteo D.L. Dalla Vedova [(2)], Paolo Maggiore [(3)], Cristian Secci [(4)],

[(1)] *Politecnico di Torino, c.so Duca degli Abruzzi 24, 10129 Turin, IT, Email: pier.berri@polito.it*
[(2)] *Politecnico di Torino, c.so Duca degli Abruzzi 24, 10129 Turin, IT, Email: matteo.dallavedova@polito.it*
[(3)] *Politecnico di Torino, c.so Duca degli Abruzzi 24, 10129 Turin, IT, Email: paolo.maggiore@polito.it*
[(4)] *Politecnico di Torino, c.so Duca degli Abruzzi 24, 10129 Turin, IT, Email: cristian.secci@studenti.polito.it*

KEYWORDS: Prognostics, Health Management, Optical Sensors, Fiber Bragg Gratings (FBG)

ABSTRACT:

Upcoming space missions will be characterized by longer duration, higher level of autonomy of the spacecraft and more extensive human presence. These aspects require robust and reliable health monitoring strategies in order to extend the spacecraft operations, increase safety of manned missions and adaptively tailor extended mission profiles according to the actual system health condition. In this context, Prognostics and Health Management (PHM) provide useful tools to determine the system health, estimate its Remaining Useful Life (RUL) and adjust operations to avoid overstressing components.

In order to gather the necessary information from the monitored system and estimate its actual health condition and RUL, a distributed network of sensors is needed, measuring heterogeneous quantities with high accuracy and high spatial resolution. Traditional technologies usually require invasive and heavy installations, and prevent fully leveraging the potentialities of PHM algorithms. In this work, we propose the use of optical sensors for strain, temperature and vibration monitoring; an experimental campaign has been carried out to validate this technology, and the results are compared with traditional sensing techniques.

1. INTRODUCTION

Optical sensors based on Fiber Bragg Gratings (FBGs) allow measurements of several heterogeneous quantities with minimal invasivity and a very small form factor [1-6].

The FBG is a section of an optical fiber, extended for a few millimeters, where a periodical modulation of the refraction index is produced through the exposure to a high power UV laser. The fiber for FBG manufacture is usually made of a germanium-doped glass: this material is photosensitive, and its refraction index can be modified by high intensity UV radiation. The grating behaves as a wavelength-specific dielectric mirror: a particular wavelength is reflected by the FBG, while the others are transmitted. The reflected wavelength λ_B is related to the grating pitch Λ_G and refraction index n:

$$\lambda_B = 2n\Lambda_G \qquad (1)$$

The operation of the FBG is based upon the Fresnel reflection [5, 6]. Every time the incident radiation crosses the interface between two different refraction indexes, it is in part transmitted and in part reflected. If the incident wavelength is close to λ_B, the reflected wave fronts are in phase, interfere constructively and light is reflected. Otherwise, the reflected wave fronts are out of phase and cancel out via destructive interference.

This phenomenon allows for the production of a sensor of temperature and strain. Mechanical strain and temperature variation influence both the effective refraction index and axial pitch of the fiber, modifying the reflected wavelength. This dependency is expressed by the following equation:

$$\Delta\lambda_B = K_\varepsilon \Delta\varepsilon + K_T \Delta T \qquad (2)$$

where ε is the mechanical strain, T is the system temperature, K_ε is the coefficient of strain, and K_T is the coefficient of temperature. During the operation of the sensor, the interrogating device uses a narrow bandwidth swept frequency laser to send a variable wavelength through the fiber. A photodetector measures the reflected spectrum to identify the peaks corresponding to the FBG wavelengths. A variation from the nominal reflected wavelength can be then addressed either to a variation in temperature or to a mechanical strain on the sensor. The two effects can be decoupled with various technique, for example relying on an additional, free-floating sensor to which no mechanical load is applied. The accuracy of the system, as well as the maximum sampling frequency and number of sensors on a single fiber, are limited primarily by the interrogating device. Typical values of sampling frequency are in the order of 25 kHz for a single sensor per channel.

Multiple sensors can be stacked on the same channel, provided their nominal wavelength is sufficiently spaced; in this case, the sampling frequency is shared among the different sensors. The number of sensors that can be stacked depends on the range of measurements (to determine the minimum wavelength spacing between two adjacent sensors) and on the total bandwidth available from the interrogator: usually, several tens to several hundreds of sensors can be placed on a single fiber, with a total length up to several kilometres. The accuracy and resolution of measures depends on the bandwidth on the laser and on the postprocessing algorithms employed. Typical values are in the order of 1pm in wavelength, corresponding to about 1 microstrain or 0.1K. The use of FBGs for prognostic monitoring of equipment has several advantages over more traditional technologies [7]. The sensors have no electronic components except for the interrogator (which can be placed up to a distance of several kilometers from the sensors), so the system is virtually insensitive to electromagnetic disturbances. The sensors are made of doped glass, being therefore robust to harsh environments (e.g. presence of aggressive chemicals, large temperature variations, outgassing phenomena, etc.) [1]. The system provides high accuracy and a flexible installation, since the sensors can be inscribed onto a single optical fiber. On the other hand, the main disadvantages are the high cost of the interrogator (which however is constantly decreasing as the TRL of the technologies advances) and the low mechanical strength of the optical fiber, which requires a very careful handling during manufacture and installation. In this paper we show an experimental campaign intended to validate the operation of FBG sensors for aerospace applications, for measures of mechanical strain, vibrations, and temperature. A first thermal and mechanical characterization of the sensors [8] has been performed in a test facility, as well as the assessment of various installation techniques [9]. Several sensors have been installed and tested on multiple composite and metal components, and the measurements have been compared to traditional sensors, such as strain gages and thermistors, and to numerical simulations.

Flight tests are planned exploiting an existing UAV platform, to prove the effectiveness of a self-contained structural monitoring equipment for aerospace vehicles. Similar system architecture will be applicable, for example, to the vibration monitoring during launch or to thermal measurements throughout the mission.

2. STATIC AXIAL STRAIN TESTS

FBG based sensors are primarily meant as optical strain gages. They provide similar accuracy as traditional components, but allow for a much less invasive installation.

A first experimental campaign was intended as an assessment of FBG strain sensors with different installation techniques. Some preliminary results were initially presented in [7].

2.1. Experimental setup

In a first experimental setup, schematically shown in Fig. 1, an optical fiber equipped with a single FBG was installed between a fixed stand and a micrometric linear actuator, with different techniques. In particular, mechanical clamping with a rubber layer was compared with gluing with epoxy resin and cyanoacrylate.
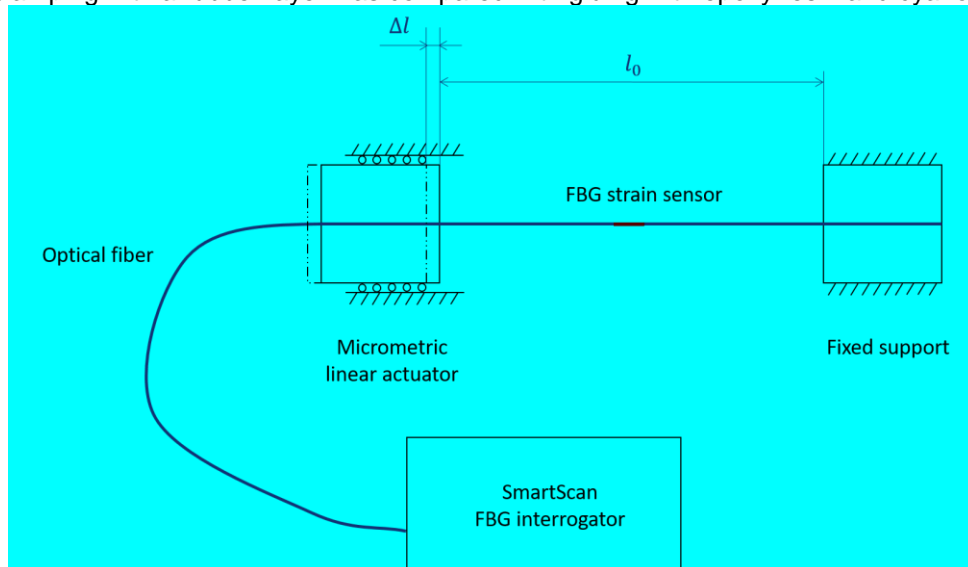

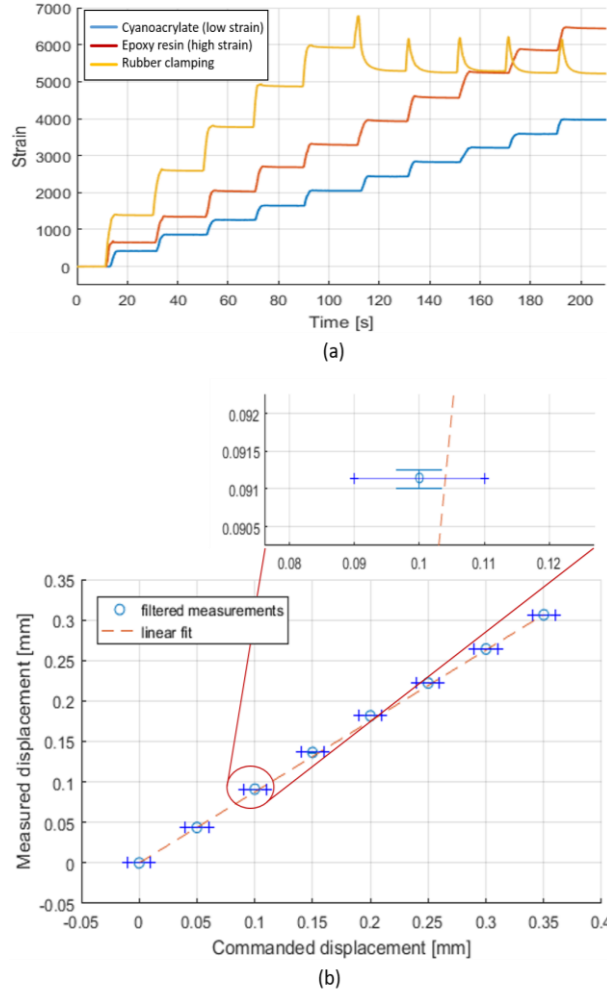*Figure 1: Experimental setup for FBG strain sensor calibration*

Figure 2: (a) comparison between rubber clamping of the fiber and gluing with cyanoacrylate and epoxy resin. (b) comparison between measured and imposed displacement.

A small displacement Δl was imposed with the linear actuator to one end of the fiber; then, as the axial stiffness of the fiber is uniform along its length, the strain can be computes as:

$$\varepsilon = \frac{\Delta l}{l_0} \tag{3}$$

where l_0 is the initial length of the fiber at rest. The computed strain is then compared to the measured one: the main source of discrepancy is identified as the deformation of the connection between the fiber and its supports.

2.2. Results of static axial strain tests

The comparison of several installation techniques showed that mechanical clamping with a rubber layer is only feasible for low strain values. At a strain in the order of 5000 µε or higher, slipping occurs between the optical fiber and the rubber layer (Fig. 2a). The exact value of strain to produce a slipping depends on the tightening pressure of the clamping; however, an excessive pressure may result in permanent damage to the rubber and optical fiber. On the other hand, bonding with glue provides better performance to the sensor up to high strain values.

Since the glue layer accounts for a significant fraction of the total displacement (even in the order of 10%), the compensation of glue elasticity cannot be neglected during data postprocessing. This discrepancy is highlighted by the comparison between measured and imposed displacement in Fig. 2b. The actual strain is determined applying to the raw sensor reading a correction, previously determined through a calibration process.
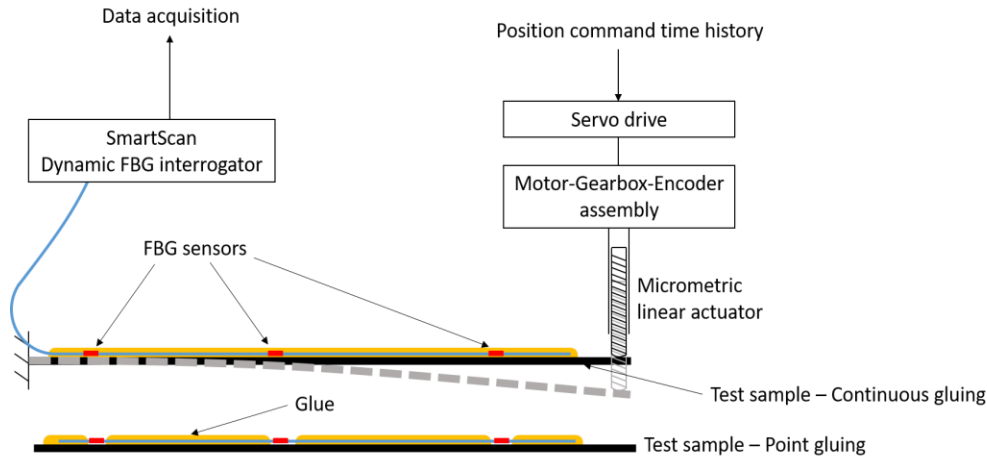
Figure 3: Experimental setup for strain measurement. The test sample is either an aluminum or composite beam with rectangular cross section.

3. STATIC BENDING TESTS

The installation described in Section 2.1 is useful for sensor calibration in laboratory environment, but is not practical for measurements on a structural component. The unprotected section of the fiber between the supports can be easily damaged with improper handling, and the installation is large and invasive.

3.1. Setup for bending tests

A more realistic installation is simulated in the experiment of Fig. 3. Here the FBG sensor is glued on a composite or aluminum sample beam involved in a bending test. A linear actuator imposes a displacement to the tip of the beam, resulting in a strain field that can be predicted quite reliably with FEM analysis.
The strain sensed by the FBG is then compared to traditional resistive strain gages and the FEM prediction.

3.2. Results of static bending tests

Several techniques for gluing were considered. Specifically, as regards the application of glue, we compared continuous and point gluing (see Fig. 3). Previous works [7, 10] highlighted how the point gluing provides no significant advantages to continuous gluing, as the accuracy of measurements is unchanged. On the other hand, continuous gluing provides a better protection of the fiber from accidental mechanical damages, since no section of the fiber is left uncovered.
As regards the curing of the glue, we tested two techniques:
-   vacuum curing of the glue with the standard setup for lamination of composite materials (employing a mold, peel ply, and vacuum bag)
-   vacuum curing without the peel ply
Two main sources of measurement errors were identified in [7, 10]. The first is the uncertainty in the thickness of the glue layer, and introduces a significant error in the measures as the glue thickness is difficult to control and is non-negligible with respect to the half-thickness of the beam. This error becomes particularly significant due to the geometry of the test samples employed for this experimental campaign. Most real application will involve components with larger characteristic dimensions (i.e. their thickness will be much bigger than that of the glue layer and sensor height), so this component of uncertainty will be greatly reduced. The second source of error can be identified in the compliance of the bonding between surface and sensor and results in an incomplete transmission of the strain of the structure to the FBG, since some of said strain is compensated by the deformation of the glue. Fig. 4 shows the readings of the FBG sensors and Strain Gages (SGs). In Fig 4 (a) the optical fiber is glued with the first strategy (with peel ply), while in Fig 4 (b) no peel ply has been used. The second strategy resulted in the best performance, providing a stiffer connection between the sensor and structure, and allowing a better control over the thickness of the glue layer: as shown in Fig 4, the FBG readings in this case are much closer to the measures from the SGs. In fact, microscope observations confirmed that with the first gluing procedure, the removal of the peel ply strips off much of the glue on and around the optical fiber, resulting on one hand in a very thin glue layer, but on the other hand in an almost unprotected fiber and in an excessively compliant connection
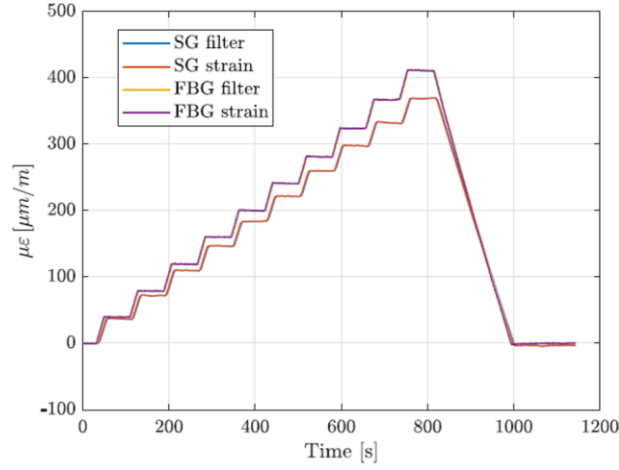
(a)
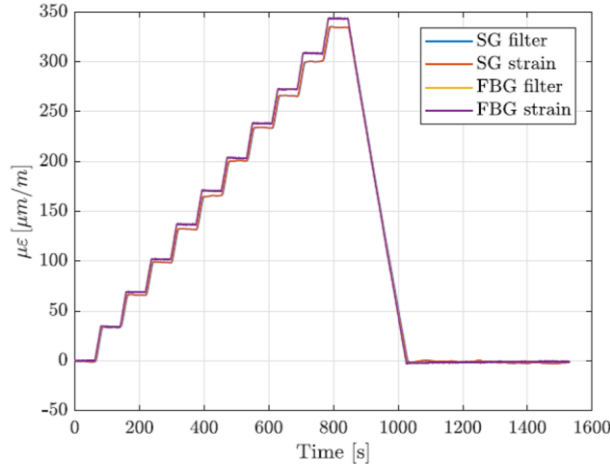
(b)

Figure 4: Comparison between Strain Gage (SG) and FBG readings, for step load application and different gluing techniques: (a) vacuum curing with peel ply; (b) vacuum curing without peel ply.

4. REPEATABILITY TESTS

Repeatability tests were performed with the same setup of Figure 1. This allowed avoiding the uncertainty due to glue thickness experienced in the second test campaign.

The same tests were repeated over the duration of one month on the same fiber, showing the dependency upon ambient temperature, humidity and glue aging. The results of this test campaign allowed a better compensation of thermal and hygroscopic effects, to achieve accurate measurements on field [11, 12].

4.1. Results of repeatability tests

The repeated application of a step deformation to the sensor showed a viscous-elastic behavior of the glue, with a characteristic time in the order of one minute (Fig. 5a). The component of deformation which is lost due to viscous yielding is recovered with the same characteristic time after the load is removed. At a constant tip displacement, the main deviation from a static sensor reading can be easily correlated to the variation of ambient temperature (which is roughly controlled by the HVAC of the test facility). This effect, visible in Fig. 5c (left), can be easily compensated through a linear regression (Fig. 5b). The proportionality coefficient resulting from the regression is compatible with the combined effects of dependency of fiber refraction index from temperature, and thermal expansion of the test stand (green curve of Fig. 5b). The residual variation from the static measure is found to be similarly correlated with environmental humidity. The effect can be compensated with the same strategy adopted for the thermal expansion, and must be addressed to the hygroscopic deformation of the glue and some polymeric components of the test stand (produced by FDM additive manufacturing in PLA), as the other components are metal. However, this effect can be estimated only from the experimental data, but is difficult to quantify with a physical model since the uncertainty in materials behavior and manufacturing tolerances is large.

5

After compensation of thermal and hygroscopic components of the deformation, a viscous creep of the glue appears, as shown in Fig. 5c, with a characteristic time in the order of 1 day. Apparently, the creep ceases after one week from the initial polymerization of the glue.

We are currently repeating these tests with higher resolution and an all-metal setup to achieve better measurements of the thermal and hygroscopic strain, and to eliminate the possible hygroscopic behavior of PLA supports.
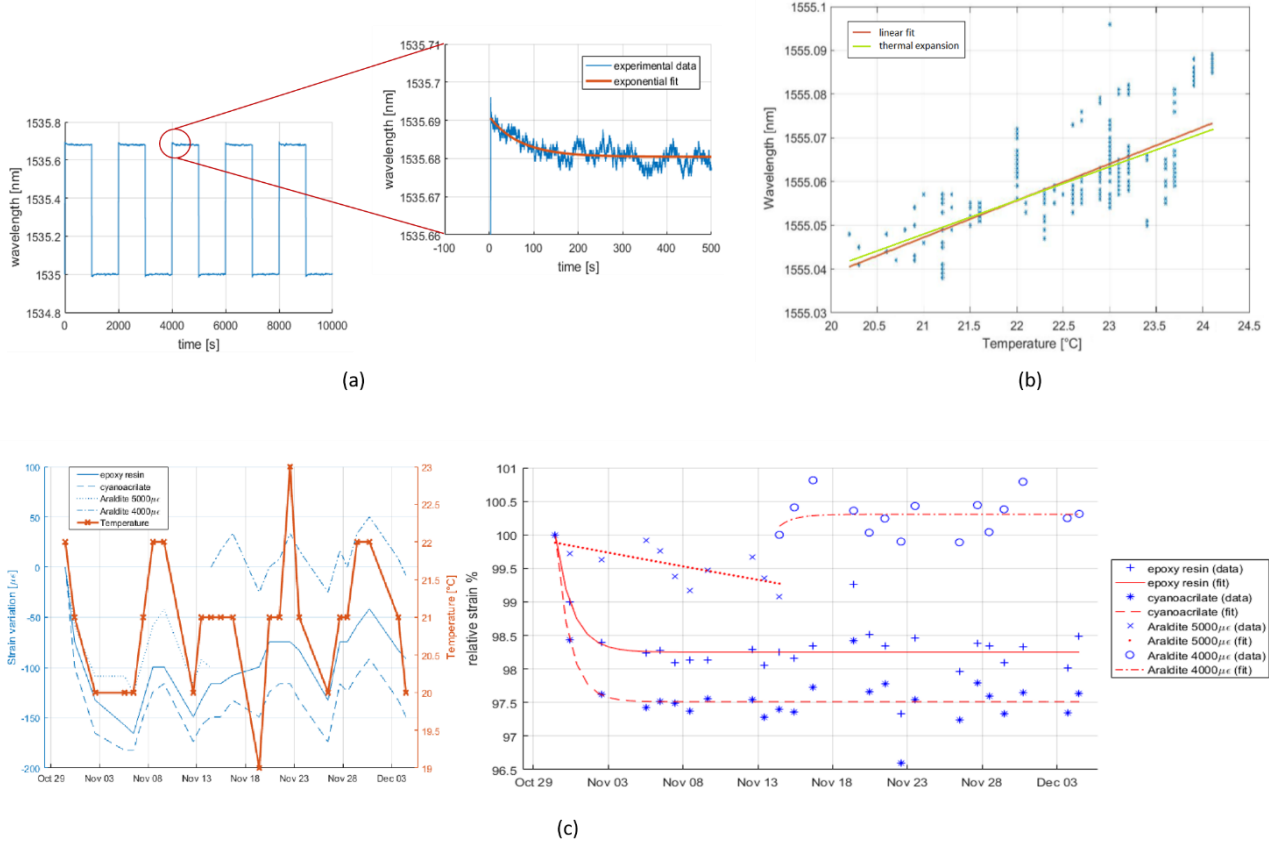

(a)

(b)

(c)

Figure 5: Results of repeatability tests. (a): viscous-elastic behavior in response to a step command; (b) linear regression for compensation of temperature-induced strain; (c) time history of raw measurements (left) and temperature and humidity compensated measurements (right).

5. THERMAL TESTS

Another possible employment of FBG based sensors for space systems monitoring and control is the measurement of temperature. The grating is sensitive to temperature through two separate physical phenomena: dependency of the refraction index on temperature and thermal expansion. While the former effect is determined and fixed for a given sensor, the other is influenced by the installation: that is, if the fiber is free-floating, it will be sensitive to its own thermal expansion coefficient; otherwise, it will be affected by the expansion of the support. Thermal measures are also needed for the compensation of strain measures: in fact, if strain measures are performed outside of a controlled laboratory environment, temperature variations will affect the accuracy of strain acquisition. This effect can be compensated by adding to the system a temperature sensor to determine the thermal component of the measured strain.

5.1. Setup for thermal tests

The setup for thermal tests, as shown in Fig. 6, consists in a Peltier Cell, controlled by a feedback loop employing a PID logic; this allows to provide an accurately regulated temperature to the FBG. The cell is enclosed in a PLA support that also acts as thermal insulation, and mounted on an aluminium baseplate/heatsink. The FBG sensor is placed directly in contact with the Peltier cell, alongside with a PT-100 resistance temperature detector employed both as a feedback for temperature control and as a reference for comparison with the FBG reading. The whole assembly is clamped by an aluminium pressure plate, to guarantee thermal continuity between the Peltier cell, FBG, and PT-100. A rubber layer is interposed between the pressure plate and the sensors to protect the sensors themselves from excessive mechanical stresses; additionally, this rubber layer allows for thermal insulation of the assembly, simplifying the thermal control.

5.2. Results of thermal tests

Several tests were performed, applying a given time-history as a command to the temperature control loop. It was observed that the best correlation between the PT-100 and FBG measurements was achieved with a succession of temperature steps, which duration of 60 seconds was intended to allow the system reach a steady sate condition. In fact, the two temperature sensors are characterized by a different time constant, the FBG being more responsive. As a result, a good matching is reached only in quasi-stationary conditions.

Due to the installation technique employed for this test, the thermal expansion experienced by the FBG is a combination of the thermal expansions of the fiber, the upper face of the Peltier cell, and the protective rubber layer. For this reason, an experimental calibration was needed.

Fig. 7 (a) shows the wavelength reflected by the FBG sensor, correlated with the reference temperature signal provided by the PT-100. The calibration was carried out in a three steps procedure:

- First, the steady state intervals were isolated from the signal, by filtering out the transients and overshoot peaks;
- Second, an average value was computed for each steady state condition, both for the PT-100 and for the FBG measurements;
- Third, a calibration curve was computed through a linear regression on the averaged data.
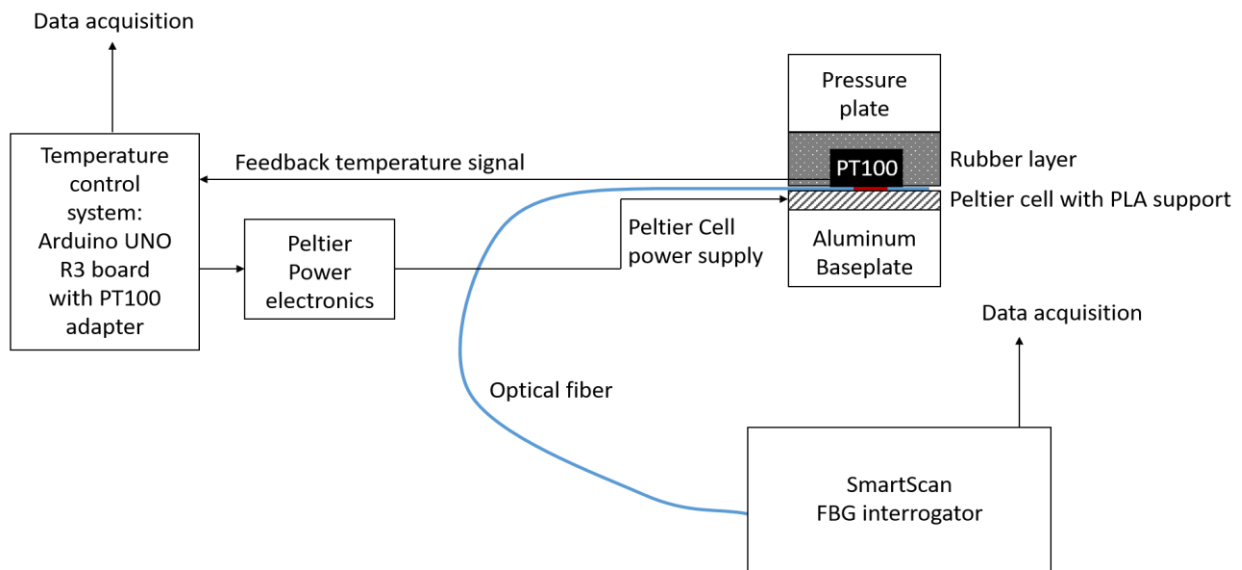

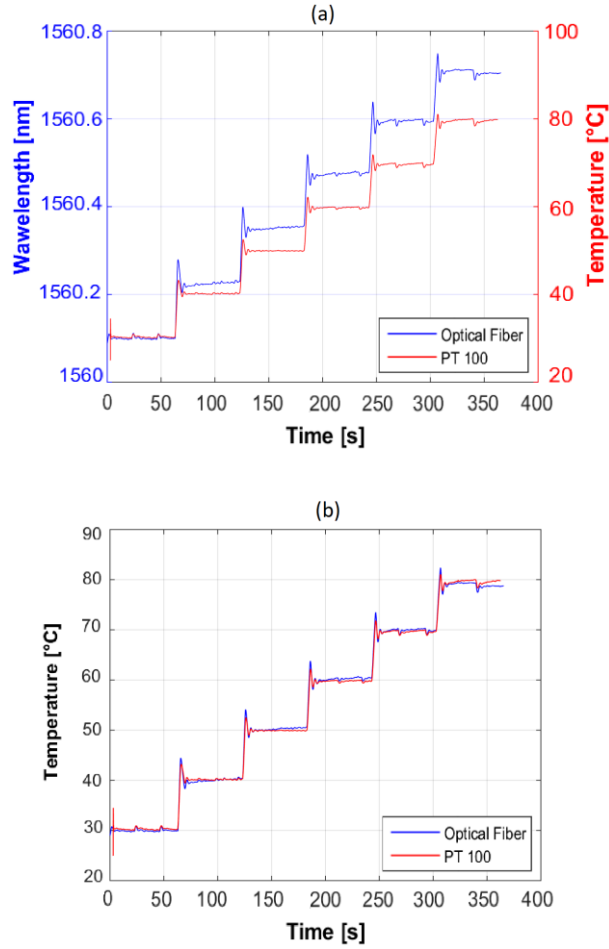*Figure6: Experimental setup for thermal tests.*

Figure 7: (a) wavelength reflected by the FBG and reference temperature signal from the PT-100. (b) comparison of the two signals after FBG calibration.

The result of the calibration is shown in Fig. 7 (b). The observed matching between the two signals is good in the steady-state sections. The discrepancy in the amplitude of the overshoot peaks can be ascribed to the different dynamic responses of the two sensors: specifically, the FBG is much smaller and lighter than the PT-100, resulting in a greatly reduced thermal capacity [13-16], a shorter time constant, and a faster response. This effect allows to follow more accurately the temperature profile during the transients, where the PT-100 behaves as a low-pass filter reducing the overshoot. The fast response of an FBG temperature sensor can be useful in several situations: for example, it could detect early an overtemperature condition on electronic equipment, and allow taking on corrective actions before permanent damage may occur. Additionally, this technology can be leveraged where an accurate measure of the temperature of a flowing fluid is needed: the temperature variations due to convective heat transfer can be followed easily despite their fast dynamics. The small discrepancies between the two sensors in steady state condition are likely due to imperfections in the contact at the interface between the face of the Peltier cell and the sensors: this results in slightly different thermal conductivity. Additionally, the PT-100 and FBG are located some millimetres apart, and their readings may be affected by a non-uniform surface temperature on the Peltier cell.

6. CONCLUSIONS

FBG based sensors were assessed to provide several measurements with a more robust and less invasive installation compared to traditional technologies. For upcoming space missions, such sensors can be employed to monitor multiple functioning parameters of the spacecraft, from launch stresses, to operating temperatures, to vibrations caused by aging mechanical equipment (e.g. reaction wheels, actuators, robotic arms, etc.) Several tests were performed, intended to test the sensors accuracy in different scenarios and measuring different heterogeneous physical quantities. The technology seems promising for the application in the harsh environment of space, given its inherent robustness to radiation, electromagnetic disturbances, temperature variation, outgassing and aggressive chemicals. The main downsides are the lack of mechanical strength, requiring a very careful handling during installation and maintenance, and the limitations on minimum curvature radius of the fiber, which may take up significant space in some

configurations of the installation.
Future developments will include flight tests with a UAV platform to test a self-contained, remotely controlled system including sensors, interrogator, data storage and telemetry equipment, facing restrictive space and weight constraints.

ACKNOWLEDGEMENTS

7. REFERENCES

1. Mihailov, S.J. (2012). Fiber Bragg grating sensors for harsh environments. *Sensors* **12(**2), 1898–1918

2. Mihailov, S.J., Grobnic, D., Hnatovsky, C., Walker, R.B., Lu, P., Coulas, D. & Ding, H. (2017). Extreme Environment Sensing Using Femtosecond Laser-Inscribed Fiber Bragg Gratings, *MDPI Sensors* **17**(12) 2909

3. Habel, J., Boilard, T., Frenière, J.S., Trépanier, F. & Bernier, M. (2017) Femtosecond FBG written through the coating for sensing applications, *MDPI Sensors* **17**(11) 2519

4. Grobnic, D., Mihailov, S., Smelser, C.W. & Ding, H. (2004). Sapphire Fiber Bragg Grating Sensor Made Using Femtosecond Laser Radiation for Ultrahigh Temperature Applications, *IEEE Photonics Technology Letters* **16**(11) 2505-2507

5. Santos, J.L. & Farahi, F. (2018). Handbook of Optical Sensors, *CRC Press*.

6. Ahuja, D. & Parande, D. (2012). Optical sensors and their applications, *J. of Scientific Research and Reviews* **1**(5) 060-068

7. Berri, P.C., Dalla Vedova, M.D.L., Maggiore, P. & Scolpito, T. (2019). Feasibility study of FBG-based sensors for prognostics in aerospace applications*, Journal of Physics: Conference Series* **1249**, 012015

8. Tanaka, N., Okabe, Y. & Takeda, N. (2003). Temperature-compensated strain measurement using fiber Bragg gratings sensors embedded in composite laminates. *Smart Mat. & Struct.* **12**(6), 940–946

9. Zhang, Y., Zhu, L., Luo, F., Dong, M., Yang, R., He, W. & Louet, X. (2016). Comparison of Metal-Packaged and Adhesive-Packaged Fiber Bragg Grating Sensors, *IEEE Sensors Journal*, **16**(15), 5958-5963

10. Berri, P.C., Dalla Vedova M.D.L., & Maggiore, P. (2019). Experimental Comparison of Fiber Bragg Grating Installation Techniques for Aerospace Systems, *MATEC Web of Conferences* **304**, 04012

11. Zhang, Y., Zhu, L., Luo, F., Dong, M., Yang, R., He, W. & Louet, X. (2016). Comparison of Metal-Packaged and Adhesive-Packaged Fiber Bragg Grating Sensors, *IEEE Sensors Journal* **16**(15) 5958-5963

12. Tanaka, N., Okabe, Y. & Takeda, N. (2003). Temperature-compensated strain measurement using fiber Bragg grating sensors embedded in composite laminates, *Smart Materials & Structures* **12**(6) 940–946

13. Hirayama, N. & Sano Y. (2000). Fiber Bragg grating temperature sensor for practical use, *ISA Transactions* **39**(2) 169-173

14. Jung, J., Nam, H., Lee, B., Byun, J.O. & Kim, N.S. (1999). Fiber Bragg grating temperature sensor with controllable sensitivity, *Applied Optics* **38**(13) 2752-2754 (1999)

15. Chen, W., Gassino, R., Liu, Y., Carullo, A., Perrone, G., Vallan, A. & Tosi, D. (2015). Performance assessment of FBG temperature sensors for laser ablation of tumors, *Proceedings of the IEEE International Symposium on Medical Measurements and Applications (MeMeA 2015)*

16. Zhang, D., Wang, J., Wang, Y. & Dai, X. (2014). A fast response temperature sensor based on fiber Bragg grating, *Measurement Science and Technology* **25**(7) (2014)